Electric Power Systems Research 211 (2022) 108424

Contents lists available at ScienceDirect

Electric Power Systems Research

journal homepage: www.elsevier.com/locate/epsr

Application of Thévenin equivalent sensitivity equations for reliable voltage stability assessment

Denis Osipov [a,*], Alan P.F. Ferreira [b,c], Joe H. Chow [a], Glauco N. Taranto [c], Tatiana M.L. Assis [c]

[a] Department of Electrical, Computer, and Systems Engineering, Rensselaer Polytechnic Institute, Troy, NY 12180, USA
[b] Department of Electrical Engineering, Federal Center for Technological Education – CEFET/RJ, Rio de Janeiro, Brazil
[c] Department of Electrical Engineering, Federal Universityof Rio de Janeiro - COPPE, Rio de Janeiro, Brazil

ARTICLE INFO

Keywords:
Parameter estimation
PMU measurements
Thevenin equivalent
Voltage stability assessment

ABSTRACT

In this paper, sensitivity equations for the Thévenin equivalent parameters, voltage and reactance, are derived using the duality between the Thévenin parameters from two consecutive PMU measurements. Using the sensitivity equation for the Thévenin reactance, a robust adaptive X-Th algorithm is developed aiming to extend a well-known adaptive E-Th approach by being able to accurately estimate the parameters for a wider range of loading conditions. In the performed case studies the resulting accuracy is evaluated when estimating the Thévenin parameters for large disturbances, for two sides with respect to a boundary bus, accommodating sensitivity to topology changes and nonlinearities in power systems. The results can be used for accurate voltage stability assessment using the Thévenin parameters.

1. Introduction

In today's power grids, concern regarding transmission infrastructure has been growing due to the continuing load demand increase [1]. Power systems are facing faster pace of renewable energy resource (RER) integration, when compared to new transmission lines reinforcements to support renewable energy delivery [2]. These scenarios lead the transmission networks to operate closer to their power transfer limits, threatening the secure operation of power systems, and increasing the risk of blackouts due to voltage instability, associated with the inability of the transmission system to address the load demand [3,4]. Therefore, the importance of robust online tools for real-time monitoring of voltage stability limits, which make timely mitigation actions from system operators possible, increases significantly.

One way to perform voltage stability assessment is to use measurements from synchronized phasor measurement units (PMU), that has already inspired the development of many voltage stability assessment approaches [5–16]. Approaches in [5–8] require network topology information obtained from the supervisory control and data acquisition system (SCADA), while approaches in [9–16] are solely based on synchronized measurements.

A popular approach [17] to perform voltage stability assessment is through the use of Thévenin equivalent models, which represents the behavior of an external system seen from a given electric node (bus), by a voltage source in series with an impedance, known as the Thévenin voltage ($\overline{E}_{Th}$) and Thévenin impedance ($\overline{Z}_{Th}$), respectively [18,19]. Fig. 1 shows the Thévenin equivalent voltage and impedance parameters ($\overline{E}_{Th}$ and $\overline{Z}_{Th}$), respectively, connected to a load bus.

The main idea of the approach is to accurately compute the equivalent parameters ($\overline{E}_{Th}$ and $\overline{Z}_{Th}$) from the buses of interest, keep the parameters updated as fast as possible in order to track topological changes, and then to monitor the maximum power transfer (MPT) constrained by the voltage stability limit of the system [3,4,20]. Inaccurate estimations of $\overline{E}_{Th}$ and/or $\overline{Z}_{Th}$ may lead to erroneous estimations of the voltage stability limits and power margins.

Among the aforementioned papers, the adaptive E-Th approach [12] combines many advantages for robust online voltage stability assessment, namely representation of the effects of nonlinearities due to control actions [21–23], the absence of requirement of network topology knowledge, and an estimation process requiring a window of just two measurements to update the Thévenin parameters towards the actual values [12].

Despite of the advantages of the adaptive E-Th approach, evaluating the formulations and assumptions made by the authors in [12] as shown in Section 2, confirmed by simulations results in Section 4, one can show that this approach may not be able to properly estimate the Thévenin

* Corresponding author.
E-mail address: osipod@rpi.edu (D. Osipov).

https://doi.org/10.1016/j.epsr.2022.108424
Received 3 October 2021; Received in revised form 7 April 2022; Accepted 2 July 2022
Available online 21 July 2022

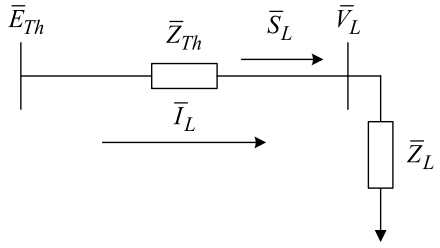

Fig. 1. Thévenin equivalent from a load bus.

parameters when the considered PMU measurements correspond to loads with a leading power factor.

To solve this issue and cover a wider range of solutions than the adaptive E-Th approach, this paper aims to provide a more comprehensive analysis of the issue of computing the Thévenin parameters in real-time adaptively and extend [12] to estimate a wider range of loading conditions, keeping the advantages of the adaptive E-Th approach. A robust approach based on the sensitivity equations for the Thévenin parameters $\overline{E}_{Th}$ and $\overline{Z}_{Th}$ is proposed, making use of the duality between the two quantities.

2. Computing the Thévenin parameters adaptively

The Thévenin equivalent of a single load connected to a stiff voltage source is shown in Fig. 1, where $\overline{E}_{Th} = E_{Th}\angle\beta$ is the Thévenin voltage phasor, $\overline{Z}_{Th} = R_{Th} + jX_{Th}$ the Thévenin impedance, $\overline{I}_L = I_L\angle 0$ the load current phasor, $\overline{V}_L = V_L\angle\theta$ the load voltage phasor, $\overline{Z}_L = Z_L\angle\theta$ the load impedance, β the angle between the Thévenin voltage and the load current, and $\theta$the angle between the load voltage and the load current.

Using Kirchhoff's voltage law, the Thévenin voltage is given by

$$\overline{E}_{Th} = \overline{Z}_{Th}\overline{I}_L + \overline{V}_L \tag{1}$$

For generators and high-voltage transmission lines $X >> R$. Hence, the assumption of $R_{Th} \approx 0$ can be made. Considering $\overline{Z}_{Th} = jX_{Th}$ and separating (1) into real and imaginary components, results in

$$\begin{pmatrix} E_{Th}\cos\beta = V_L\cos\theta \\ E_{Th}\sin\beta = X_{Th}I_L + V_L\sin\theta \end{pmatrix} \tag{2}$$

In (2) I_L, V_L, and θ are known from measurements, whereas E_{Th}, X_{Th}, β are unknown variables. In (2) $\overline{I}_L$ is used as the angle reference instead of $\overline{V}_L$ or $\overline{E}_{Th}$ because the resulting expressions are simpler to work with.

2.1. Adaptive X-Th and E-Th approaches

To solve the underdetermined system of equations in (2), two approaches can be derived: the first one choosing E_{Th} as a free variable, that will be named as "adaptive E-Th approach", and the second one selecting X_{Th} as a free variable, which will be called "adaptive X-Th approach."

For the adaptive E-Th approach, E_{Th} has its value set independently, and then β and X_{Th} are computed using the following equations, derived from (2) as

$$\beta = \arccos\left(\frac{V_L\cos\theta}{E_{Th}}\right), \quad X_{Th} = \frac{E_{Th}\sin\beta - V_L\sin\theta}{I_L}, \tag{3}$$

If the actual value is chosen for E_{Th}, then X_{Th} and β will achieve their correct values as well.

For the adaptive X-Th approach, X_{Th} is chosen independently, and then β and E_{Th} are computed using equations, also derived from (2) as

$$\beta = \arctan\left(\frac{X_{Th}I_L + V_L\sin\theta}{V_L\cos\theta}\right), \quad E_{Th} = \frac{V_L\cos\theta}{\cos\beta} \tag{4}$$

Analogously to what happens in the adaptive E-Th approach, if the actual X_{Th} is set, the correct values of β and E_{Th} can be obtained.

2.2. Estimating thévenin parameters adaptively

Both adaptive approaches (E_{Th} or X_{Th}) require conditions to properly update the free variables, after the initial guess, in order to achieve convergence to their actual values.

To solve this issue, the adaptive E-Th approach developed a theorem based on two different consecutive loading conditions, relying in the variation of the absolute value of the load impedance $\Delta Z_L^i = Z_L^i - Z_L^{i-1}$, and on the difference between two consecutive estimated values for the Thévenin reactance $\Delta X_{Th}^i = X_{Th}^i - X_{Th}^{i-1}$ using (3), to identify whether E_{Th}^i is over- or under-estimated. Once the over- or under-estimation of the free variable is identified, a predetermined sized decrement or increment, is applied to the current estimated value of E_{Th}^i. This procedure is performed for every new pair of different PMU measurements, and E_{Th}^i is updated until convergence is achieved. In short, the developed theorem increases E_{Th}^i when ΔZ_L and ΔX_{Th} have same signs, and decreases E_{Th}^i when ΔZ_L and ΔX_{Th} have opposite signs.

Nonetheless, evaluating the formulations and assumptions made by the authors in [12], confirmed by simulation results, one can show that this approach is not able to properly estimate the Thévenin parameters when the PMU measurements represent a load with leading power factor, as the one shown in Figs. 2(b), since (3) is not able to compute negative values of β, which is a possibility when the actual X_{Th} has a low value, or when the system is subjected to a light loading condition. Fig. 2 (a) and (b) reflect capacitive loading conditions for positive and negative values of β, respectively. When the load is inductive, if $\overline{I}_L$ is chosen as the phase reference, β is always positive.

Based on this observation, to extend the adaptive E-Th approach, a new adaptive approach is proposed based on the sensitivity equations for E_{Th} and X_{Th}, obtained from the analytical expressions for the Thévenin parameters when two consecutive loading conditions are considered. The role of the sensitivity equations is to provide accurate decisions for each updating step regardless of whether the E-Th or X-Th approach is chosen, to bring the initial guess for the chosen free variable towards its convergence, replacing the theorem from the adaptive E-Th

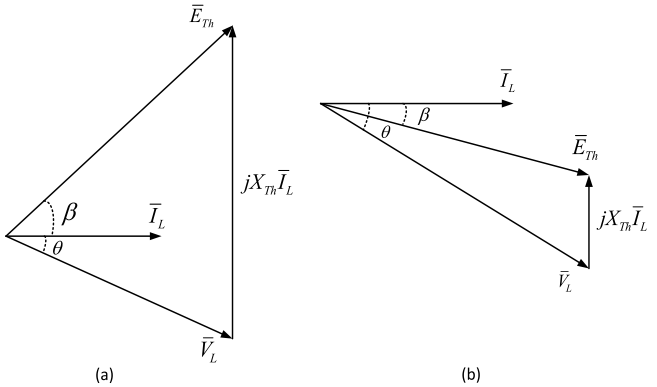

Fig. 2. Capacitive loads phasor diagrams: (a) positive β, (b) negative β.

approach but keeping its benefits.

3. Derivation of the sensisitvity equations

3.1. True Thévenin reactance and voltage solutions

Combining (3) by squaring both equations and adding them to form a single equation, one can achieve the following single β-independent equation

$$E_{Th}^2 = V_L^2 + X_{Th}^2 I_L^2 + 2X_{Th} I_L V_L \sin\theta \tag{5}$$

Eq. (5) has two unknowns: E_{Th} and X_{Th}; hence, with two sets of PMU measurements, it is possible to obtain those quantities. Substituting $Q_L = I_L V_L \sin\theta$ in (5) and using two consecutive sets of measurements with different loading conditions results in

$$\begin{pmatrix} E_{Th}^2 = \left(V_L^{i-1}\right)^2 + X_{Th}^2 \left(I_L^{i-1}\right)^2 + 2X_{Th} Q_L^{i-1} \\ E_{Th}^2 = \left(V_L^{i}\right)^2 + X_{Th}^2 \left(I_L^{i}\right)^2 + 2X_{Th} Q_L^{i} \end{pmatrix} \tag{6}$$

where i and i–1 stand for the current and previous measurements, respectively.

One can verify that (6) is formed by two quadratic equations, and theoretically, it has four pairs of solutions: four values for E_{Th} (all four solutions are unique) and four for X_{Th} (two out of four solutions are unique). Therefore, more than one solution can be obtained for the Thévenin parameters when they are estimated from two consecutive loading conditions. However, as described in the Appendix A, just one out of four pairs is related to the actual parameters.

Solving (6) two unique solutions for X_{Th} are obtained:

$$X_{Th} = \frac{Q_L^i - Q_L^{i-1} \pm \sqrt{\left(Q_L^{i-1} - Q_L^i\right)^2 - \left[\left(I_L^{i-1}\right)^2 - \left(I_L^i\right)^2\right]\left[\left(V_L^{i-1}\right)^2 - \left(V_L^i\right)^2\right]}}{\left(I_L^{i-1}\right)^2 - \left(I_L^i\right)^2} \tag{7}$$

and four (two for each X_{Th}) solutions for E_{Th} are obtained:

$$E_{Th} = \pm \frac{\sqrt{\left(I_L^{i-1}\right)^2 \left(V_L^i\right)^2 - \left(I_L^i\right)^2 \left(V_L^{i-1}\right)^2 + 2\left[\left(I_L^{i-1}\right)^2 Q_L^i - \left(I_L^i\right)^2 Q_L^{i-1}\right] X_{Th}}}{\left(I_L^{i-1}\right)^2 - \left(I_L^i\right)^2} \tag{8}$$

Negative E_{Th} solutions are not feasible for the Thévenin equivalent of a real system and can be excluded leaving only two E_{Th} solutions which correspond to two X_{Th} solutions.

From (7) and (8) it is not possible to distinguish the true and wrong solution for every new pair of PMU measurements. In addition, if the measurements are corrupted by noise, the accuracy of Thévenin parameters estimation can be affected, which in turn can hinder voltage stability assessment.

3.2. Sensitivity equations for the X-Th and E-Th approaches

To identify the actual solution correctly, the sensitivity equations (for both X-Th and E-Th approaches) are developed. The sensitivity expressions drive the updates from an initial guess for the free variables toward the actual parameter values, with increments or decrements for every new available measurement.

Define $E_{Th} = E_{Th}^{app} + \Delta E_{Th}$ and $X_{Th} = X_{Th}^{app} + \Delta X_{Th}$, where E_{Th}^{app} and X_{Th}^{app} are the approximate Thévenin parameters and ΔE_{Th} and ΔX_{Th} are the approximate differences between the true and approximate Thévenin parameters, and assume that $\Delta E_{Th}^2 \approx 0$ and $\Delta X_{Th}^2 \approx 0$. When E_{Th} and X_{Th} are squared, the following expressions are obtained

$$\begin{aligned} E_{Th}^2 &= \left(E_{Th}^{app}\right)^2 + 2E_{Th}^{app} \Delta E_{Th}, \\ X_{Th}^2 &= \left(X_{Th}^{app}\right)^2 + 2X_{Th}^{app} \Delta X_{Th} \end{aligned} \tag{9}$$

yielding approximated expressions for the true E_{Th}^2 and X_{Th}^2.

Substituting the approximate expressions for E_{Th}^2 and X_{Th}^2 from (9) into (6) and solving for ΔX_{Th} results in

$$\Delta X_{Th} = -X_{Th}^{app} - \frac{1}{2} \frac{\left(X_{Th}^{app} I_L^i\right)^2 - \left(X_{Th}^{app} I_L^{i-1}\right)^2 + \left(V_L^{i-1}\right)^2 - \left(V_L^i\right)^2}{X_{Th}^{app}\left(I_L^{i-1}\right)^2 - X_{Th}^{app}\left(I_L^i\right)^2 + Q_L^{i-1} - Q_L^i} \tag{10}$$

Rearranging and simplifying (10) using (5), results in

$$\Delta X_{Th} = \frac{E_{Th}^i - E_{Th}^{i-1}}{\frac{Q_S^{i-1}}{E_{Th}^{avg}} - \frac{Q_S^i}{E_{Th}^{avg}}} = E_{Th}^{avg} \frac{\left(E_{Th}^i - E_{Th}^{i-1}\right)}{\left(Q_S^{i-1} - Q_S^i\right)} \tag{11}$$

where E_{Th}^i and E_{Th}^{i-1} are computed from (4), $E_{Th}^{avg} = \frac{E_{Th}^i + E_{Th}^{i-1}}{2}$, $Q_S^i = X_{Th}^{app}\left(I_L^i\right)^2 + Q_L^i$ and $Q_S^{i-1} = X_{Th}^{app}\left(I_L^{i-1}\right)^2 + Q_L^{i-1}$ are the approximated reactive power values from the voltage source.

Eq. (11) highlights that $(E_{Th}^i - E_{Th}^{i-1})$ and $(Q_s^{i-1} - Q_s^i)$ are the key factors that the sign of the increment ΔX_{Th} depends on, i.e., it depends on the source reactive power difference and the computed equivalent voltage difference.

Using the duality between E_{Th} and X_{Th}, a similar sensitivity equation can be obtained as

$$\Delta E_{Th} = \frac{X_{Th}^i - X_{Th}^{i-1}}{\frac{E_{Th}^{app}}{Q_s^{i-1}} - \frac{E_{Th}^{app}}{Q_s^i}} = -\frac{\left(Q_s^{i-1} Q_s^i\right)}{E_{Th}^{app}} \frac{\left(X_{Th}^i - X_{Th}^{i-1}\right)}{\left(Q_s^{i-1} - Q_s^i\right)} \tag{12}$$

where E_{Th}^{app} is the free variable, and X_{Th}^i and X_{Th}^{i-1} are computed from (3).

Comparing (11) and (12), one can verify that regardless of the approach, the source reactive power difference is the key factor for the sign of the increment, and for the adaptive E-Th approach the sign of the increment depends on $(X_{Th}^i - X_{Th}^{i-1})$, instead of $(E_{Th}^i - E_{Th}^{i-1})$.

Reaching this point, the adaptive E-Th approach sensitivity Eq. (12) falls into the same limitation described in Section II.B for the method in [12], which is not guaranteed to compute the sign of β correctly, when the actual sign is negative. Thus, besides the sensitivity equation, the adaptive E-Th approach would also require an additional algorithm to detect the sign of β correctly.

However, this limitation is not present in the system of Eq. (4) of the adaptive X-Th approach. In this case the sign of β can be calculated correctly because arctan is an odd function. Thus, the adaptive X-Th approach sensitivity equation is chosen to develop a robust algorithm to estimate the Thévenin parameters in real-time.

3.3. Convergence to the true solution

In order to assure that the sensitivity Eq. (11) leads the estimated parameters toward the actual quantities, the initial guess should be chosen as lying in a feasible operational range of values, following similar procedures as in [12]. Choosing the actual value lying between zero and the load impedance Z_L^i, the initial X_{Th} value is set as

$$X_{Th}^0 = \frac{Z_L^0}{2} \tag{13}$$

If the initial guess for X_{Th} is outside of the aforementioned feasible range, the algorithm may converge to the wrong solution of (6).

3.4. Algortithm for the adaptive X-Th approach

As described in Section III.B the sign of Eq. (11) depends on the source reactive power difference $(Q_s^{i-1} - Q_s^i)$, and the difference $\Delta E_{Th}^{app} = (E_{Th}^i - E_{Th}^{i-1})$.

Thus, to promote a robust approach against measurement noise, instead of using both the increment and direction provided by (11), only the direction from (11) is used, because due to noise-related errors infeasible increments may be computed, possibly leading to a non-convergent estimation. For the increments, a pre-fixed step size is

chosen, following the same choice used in [12].

The formulations described in Sections III.B – III.C are combined to establish the following algorithm:

(1) Set the increment constant k_{inc}.
(2) Compute X_{Th}^{0} using (13).
(3) Compute (β^{i}, E_{Th}^{i}) using X_{Th}^{i-1} in (4).
(4) Compute $\Delta E_{Th} = E_{Th}^{i} - E_{Th}^{i-1}$.
(5) Compute $\Delta Q_s = Q_S^{i-1} - Q_S^{i}$.
(6) Compute the increment $\Delta X = X_{Th}^{i-1} k_{inc}$.
(7) Check the following conditions:
  a If $\Delta Q_s \cdot \Delta E_{Th} > \varepsilon$, then $X_{th}^{i} = X_{Th}^{i-1} + \Delta X$,
  b If $\Delta Q_s \cdot \Delta E_{Th} < -\varepsilon$, then $X_{th}^{i} = X_{Th}^{i-1} - \Delta X$,
  c Otherwise, $X_{th}^{i} = X_{Th}^{i-1}$.
(8) Update (β^{i}, E_{Th}^{i}) using X_{Th}^{i} in (4).
(9) Increment i and go back to step 3.

In the algorithm ε sets a minimum variation for $|\Delta Q_s \cdot \Delta E_{Th}|$ so that if it is sufficiently small, then the estimated parameters are not updated. For the performed simulations ε is set to 10^{-6}.

4. Case studies

4.1. 2-machine system

To show the accuracy of the new adaptive X-Th approach in estimating the Thévenin parameters, a 2-machine system shown in Fig. 3 is considered. With this system it is possible to verify the response of the new approach to topology variation, estimation during a large disturbance, and estimation when the measurements correspond to loading condition with leading power factor.

In addition, an issue raised by [18,19], which is related to estimating the Thévenin parameters from both sides with respect to a boundary bus, is addressed. The authors in [19] mention that approaches based on curve fitting, e.g., based on the least-squares error minimization, using current and voltage measurements at the boundary bus is only able to estimate one of the sides, which is called "stable side." The stable side is defined as the side with less absolute variation of their equivalent parameters during the evaluated time window. The other side, with more variation is called the "changing side." For example, if a time window of two consecutive PMU measurements is considered, the side which varies less between these two loading conditions will be estimated. However, they also mention the stable side may switch under some conditions, e.g., large penetration of variable non-dispatchable RER, which may lead methods as in [10] to track parameters from the other side. The proposed adaptive approach aims to estimate both sides independently and track possible changes from both sides in real-time.

For the system in Fig. 3, it is assumed that there are PMU measurements of voltage and current available at the boundary bus at a reporting rate of 20 measurements per second. Area 1 has a large generator, modeled as an infinite bus ($X_{gen1} \approx 0$ pu), connected to the boundary bus through two transmission lines with reactance of 0.2 pu. Area 2 has a small generator, modeled with transient dynamics and a governor, but without an excitation system. This generator has the transient reactance $X'_d = 0.31$ pu and is connected to the boundary bus via a transformer with reactance 0.15 pu. The reason for choosing such a simple test system is that the true equivalent parameters can be established analytically, and then compared to the parameters estimated by the evaluated methods.

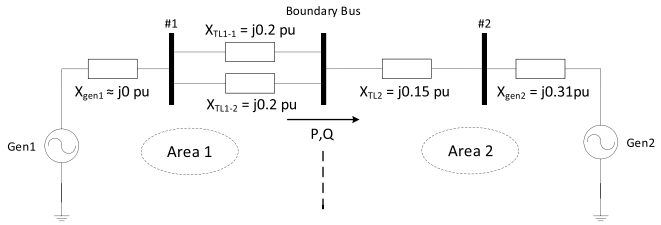

Fig. 3. Diagram of a 2-machine system.

The simulation scenario consists of a series of ramps and steps of the active power flowing from Gen 2 towards the infinite bus #1, as well as the event of tripping one of the lines connecting bus #1 to the boundary bus at 70 s, promoting a topology change. Fig. 4 shows the active and reactive power measured at the boundary bus.

To show the improvements provided by the proposed adaptive X-Th approach, two other methods are also considered, namely the adaptive E-Th approach [12] and the Recursive Least-Squares (RLS) approach [10], which is an approach based on estimation of the Thévenin parameters by curve fitting. In order for the RLS approach to make estimations for the same time window as for the proposed and the adaptive E-Th approaches, a forgetting factor of 0.5 is used for the RLS approach.

The estimated Thévenin reactances and voltages for Area 1 are shown in Fig. 5 and Fig. 6, respectively.

One can verify that the proposed approach and the RLS approach can properly estimate the Thévenin reactance of Area 1, since both methods obtain the value of 0.1 pu until 70 s, before the line is tripped, and both properly update their estimations to 0.2 pu after 70 s, showing good sensitivity to topology changes. In Fig. 6, the Thévenin voltage for Area 1 is correctly estimated by the proposed RLS approaches, obtaining the value of 1.0 pu. The adaptive E-Th approach is not able to estimate the actual parameters, which happens because the measurements reflect a leading power factor scenario.

Fig. 7 and Fig. 8 show the estimated Thévenin reactances and voltages for Area 2, respectively.

The adaptive E-Th approach properly estimates Area 2 side because in this case the PMU measurements reflect a positive active and reactive power, a scenario for which the

E-Th approach was designed. The RLS approach converges to the negative values of the Area 1 parameters and is not able to track the correct parameter values of Area 2 most of the time.

When estimating the Area 1 parameters, according to [19] the RLS approach correctly converges to the actual parameters because Area 1 is the stable side for most of the evaluated two-measurements time windows, which means the Area 1 parameters provide an estimation with smaller squared errors. Nonetheless, for the specific time range between 70 s and 70.05 s another value is estimated, which is the negative of the equivalent reactance of Area 2, a value close to 0.46 pu. This result is also consistent with the derivations in [19], meaning that Area 2 becomes the stable side for this time span due to the line trip in Area 1, making Area 1 the changing side. The negative sign of estimated reactance comes from the fact the stable side (the estimated side) is the side the considered current is directed to, i.e., from Area 1 to Area 2. Similar situation happens when the Area 2 parameters are estimated by RLS

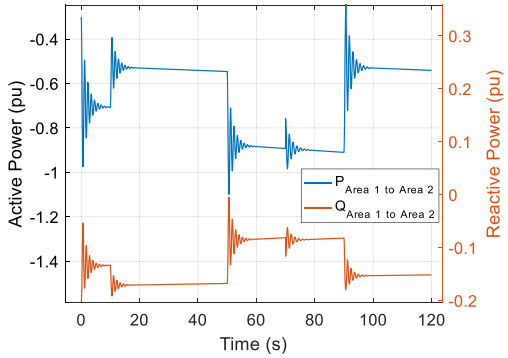

Fig. 4. Active and reactive power measured at the boundary bus.

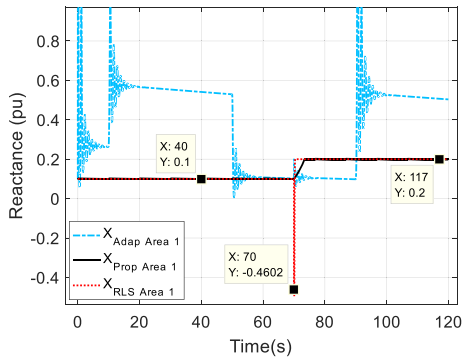

Fig. 5. Thévenin reactances of area 1.

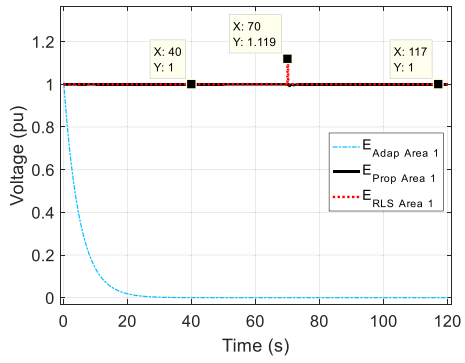

Fig. 6. Thévenin voltages of area 1.

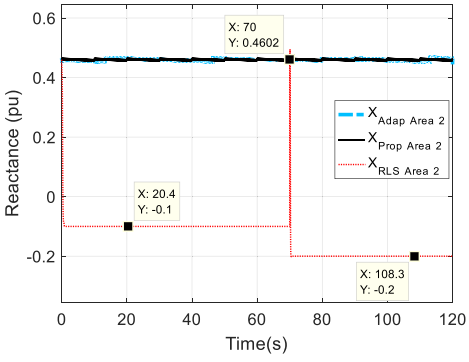

Fig. 7. Thévenin reactances of area 2.

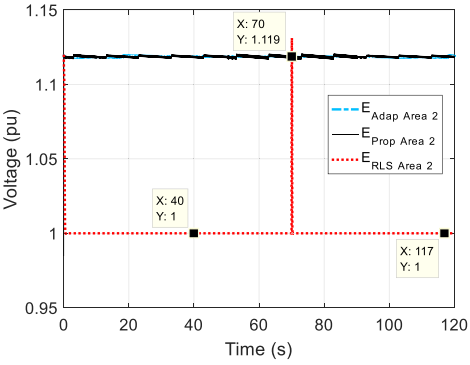

Fig. 8. Thévenin voltages of area 2.

approach.

4.2. IEEE 39-bus system

In this section we use a well-known New England 39-bus system representing part of the US Eastern Interconnection. The system has 10 generators and is shown in Fig. 9. The scenario of the load increase from [16] is simulated. Loads are modeled as constant power loads. Load 8 is increased by 10 MW/s keeping the power factor constant until voltage collapse occurs. The voltage magnitude and angle at bus 8, the active and reactive power on lines connecting to bus 8 (lines 8–5, 8,7 and 8,9) are recorded at 30 measurements per second and used as PMU measurements. The system data can be found in [24].

The estimated Thevénin reactance together with the equivalent load impedance are shown in Fig. 10.

In Fig. 10 at about 3.8 s X_{prop} converges to a value close 0.02 pu, being subjected to two step changes before the impedance matching happens: one at about 60 s and the other at about 150 s, which is consistent with the system events, since the generators G2 (bus 31) and G3 (bus 32) reach their over-excitation limits (OELs) at those times, respectively, causing the equivalent impedance to increase because with the terminal bus voltage support loss, their internal machine reactances become part of the equivalent Thévenin reactance.

Fig. 10 reflects an accurate estimation of the Thévenin reactance X_{prop} since it properly tracks the MPT, once its impedance matches with Z_L (at 172 s) just before the active power P_L reaches its peak (at 173 s).

To demonstrate the accuracy of voltage stability assessment using estimated Thévenin parameters, a power transfer stability margin (PTSM) is introduced. PTSM is based on the maximum active power that the transmission system can provide to the load. For a lossless transmission system, where $R_{Th} = 0$, maximum active power is calculated from [4] as

$$P_{\max} = \frac{E_{Th}^2 \cos\theta}{2X_{Th}(1+\sin\theta)} \tag{14}$$

Using (14) PTSM is defined as

$$\text{PTSM} = \frac{P_{\max} - P_L}{P_{\max}} = 1 - \frac{2P_L X_{Th}(1+\sin\theta)}{E_{Th}^2 \cos\theta} \tag{15}$$

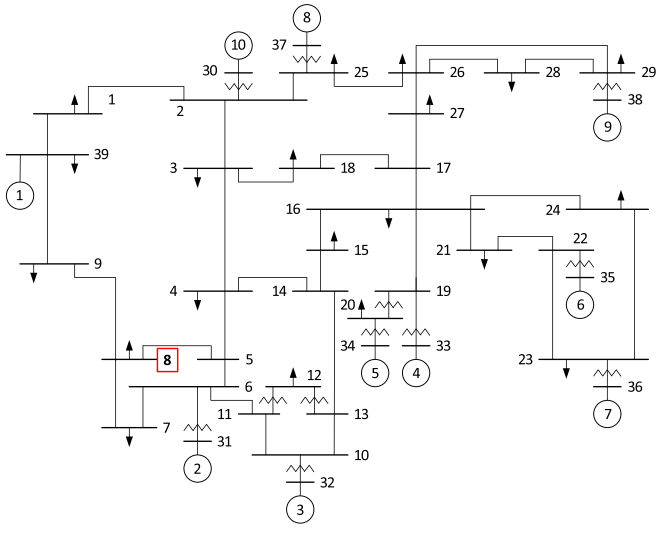

Fig. 9. IEEE 39-bus system.

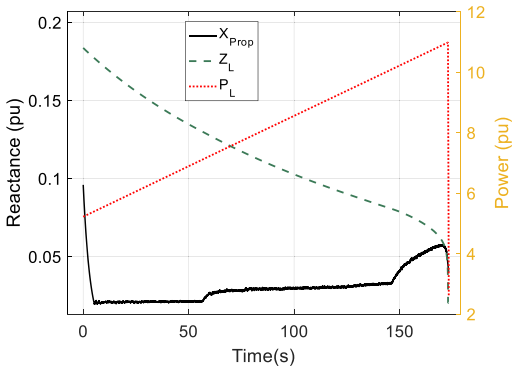

Fig. 10. Estimated Thévenin reactance from the boundary bus.

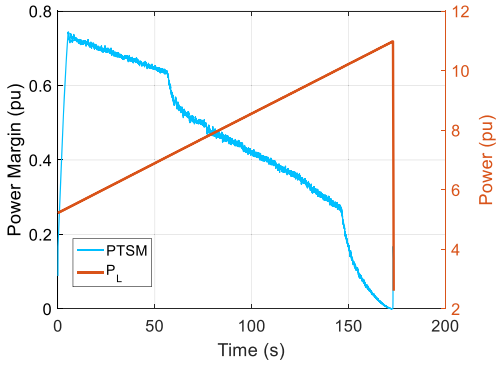

Fig. 11. Power transfer stability margin.

PSTM calculated for the 39-bus scenario is shown in Fig. 11. In Fig. 11 the increase of estimated Thévenin reactance at about 60 s and 150 s is reflected in the decrease of the margin. Thus, PTSM calculated from the estimated Thévenin parameters is sensitive to the conditions when over-excitation limits are reached. At 172 s PTSM reaches zero accurately indicating voltage instability.

It is worth mentioning that even though the resistances of transmission lines in the IEEE 39-bus system are not equal to zero [24], which is one of the assumptions considered in the proposed approach in Section 2, the proposed approach still achieves accurate tracking of the MPT, which is demonstrated in Figs. 10 and 11.

5. Conclusions

From the developed sensitivity Eqs. (11) and (12) for E_{Th} and X_{Th}, respectively, it follows that the reactive power difference at the equivalent voltage source is the key quantity to update the free variables. When the Thévenin parameters are being estimated adaptively in real-time from an initial guess, the sign of the reactive power difference ensures convergence of the Thévenin parameters to their actual values.

From the analytical solutions (7) and (8) it is shown that two possible solutions for the Thévenin equivalent parameters exist. The infeasible solution is excluded by choosing feasible initial guess for the free variable.

The proposed adaptive X-Th approach, based on the X_{Th} sensitivity equation, shows an accuracy improvement compared to the adaptive E-Th approach when both are tested in the 2-machine system case. When the considered PMU measurements represent leading power factor, the proposed approach estimates the Area 1 parameters correctly, while the adaptive E-Th approach diverges. Moreover, the proposed approach is able to properly estimate both system sides with respect to the boundary bus, while the RLS and adaptive E-Th approaches are only able to estimate one system side. Also, the proposed approach shows good performance against large disturbance and good sensitivity to topology changes.

Finally, in the test on the IEEE 39-bus system, when voltage stability assessment is performed, the proposed approach shows accurate estimation as the impedance matching condition is able to properly reflect the instability inception. In addition, the proposed approach properly responds to the effect of the nonlinearities caused by the action of the OELs of generators by updating the equivalent parameters.

6. Appendix

6.1. Example of Thévenin calculation using solution of a system of quadratic equations

To demonstrate four pairs of solutions of the system of two quadratic equations in (6) two sets of measurements in per unit from Section III.A are used:

$V_L^{i-1} = 1.0152956$, $I_L^{i-1} = 0.5531616$, $Q_L^{i-1} = 0.1694249$, $V_L^{i} = 1.0152950$, $I_L^{i} = 0.55318535$, $Q_L^{i} = 0.1694202$.

Solving (6) the following pairs of solutions are obtained

$$E_{Th} = \begin{pmatrix} -1 \\ -1.119 \\ 1 \\ 1.119 \end{pmatrix} \qquad X_{Th} = \begin{pmatrix} -0.2 \\ 0.46 \\ -0.2 \\ 0.46 \end{pmatrix} \tag{A1}$$

There is always a negative X_{Th} solution if measurements are obtained at a boundary bus (Fig. 3). The last pair of solutions correspond to true Thévenin equivalent values: $E_{Th} = 1.119$ pu, $X_{Th} = 0.46$ pu.

CRediT authorship contribution statement

Denis Osipov: Conceptualization, Methodology, Software, Writing – original draft. **Alan P.F. Ferreira:** Methodology, Software, Validation, Writing – original draft, Visualization. **Joe H. Chow:** Conceptualization, Writing – review & editing, Supervision. **Glauco N. Taranto:** Conceptualization, Supervision. **Tatiana M.L. Assis:** Supervision.

Declaration of Competing Interest

The authors declare that they have no known competing financial interests or personal relationships that could have appeared to influence the work reported in this paper.

Acknowledgment

The authors would like to thank Dr. Chengxi Liu and Dr. Fengkai Hu for providing the IEEE 39-bus system model.

This work was supported in part by the Engineering Research Center Programof the NSF and the DOE under the supplement to NSF Award Number. EEC-1041877, the CURENT Industry Partnership Program and by CNPq, FAPERJ, INERGE, FAPEMIG and Coordenação de

Aperfeiçoamento de Pessoal de Nível Superior (CAPES) Finance Code 001.

References

[1] U.S. Energy Information Administration (EIA), "Annual Energy Outlook 2021 - with projections to 2050 - Narrative,", U.S. Department of Energy, Washington, DC, 2021 [Online]. Available, https://www.eia.gov/outlooks/aeo/pdf/AEO_Narrative_2021.pdf.

[2] Electric Reliability Council of Texas (ERCOT), Report on Existing and Potential Electric System Constraints and Needs, Electric Reliability Council of Texas (ERCOT), 2019 [Online]. Available, http://www.ercot.com/content/wcm/lists/172485/2019_Constraints_and_Needs.pdf [Accessed December 2019].

[3] C.W. Taylor, Power System Voltage Stability, McGraw-Hill, Singapore, 1994.

[4] T. van Cutsem, C. Vournas, Voltage Stability of Electric Power Systems, Springer Science+Business Media, Dordrecht, The Netherlands, 1998.

[5] Y. Wang, I.R. Pordanjani, W. Li, W. Xu, T. Chen, E. Vaahedi, J. Gurney, "Voltage stability monitoring based on the concept of coupled single-port circuit,", IEEE Trans. Power Syst. 26 (4) (Nov. 2011) 2154–2163.

[6] J.H. Liu, C.C. Chu, "Wide-area measurement-based voltage stability indicators by modified coupled single-port models,", IEEE Trans. Power Syst. 29 (2) (Mar. 2014) 756–764.

[7] M. Glavic, T. Van Cutsem, "Wide-area detection of voltage instability from synchronized phasor measurements, Part I: Principle,", IEEE Trans. Power Syst. 24 (3) (2009) 1408–1416.

[8] M. Glavic, T. Van Cutsem, "Wide-area detection of voltage instability from synchronized phasor measurements, Part II: Simulation Results,", IEEE Trans. Power Syst. 24 (3) (2009) 1417–1425.

[9] K. Vu, M.M. Begovic, D. Novosel, M.M. Saha, "Use of local measurements to estimate voltage-stability margin,", IEEE Trans. Power Syst. 14 (3) (1999) 1029–1035.

[10] B. Milosevic, M. Begovic, "Voltage-stability protection and control using a wide-area network of phasor measurements,", IEEE Trans. Power Syst. 18 (1) (2003) 121–127. Feb.

[11] I. Smon, G. Verbic, F. Gubina, "Local voltage-stability index using Tellegen's theorem,", IEEE Trans. Power Syst. 21 (3) (2006) 1267–1275. Aug.

[12] S. Corsi, G.N. Taranto, "A real-time voltage instability identification algorithm based on local phasor measurements,", IEEE Trans. Power Syst. 23 (3) (2008) 1271–1279. Aug.

[13] F. Hu, K. Sun, A. Del Rosso, E. Farantatos, N. Bhatt, "Measurement-based real-time voltage stability monitoring for load areas,", IEEE Trans. Power Syst. 31 (4) (2016) 2787–2798.

[14] C.D. Vournas, C. Lambrou, P. Mandoulidis, "Voltage stability monitoring from a transmission bus PMU,", IEEE Trans. Power Syst. 32 (4) (Jul. 2017) 3266–3274.

[15] P. Mandoulidis, C. Vournas, "A PMU-based real-time estimation of voltage stability and margin,", Electr. Power Syst. Res. 178 (Jan. 2020) 1–12.

[16] C. Liu, F. Hu, D. Shi, X. Zhang, K. Sun, Z. Wang, Measurment-based voltage stability assessment considering generator VAR limits, IEEE Trans. Smart Grid 11 (1) (2020) 301–311.

[17] M. Glavic, T. van Cutsem, "A short survey of methods for voltage instability detection,", in: Proceedings of the IEEE Power and Energy Society General Meeting, Detroit, MI, 2011.

[18] S.M. Abdelkader, D.J. Morrow, "Online tracking of Thevenin equivalent parameters using PMU measurements,", IEEE Trans. Power Syst. 27 (2) (May 2012) 975–983.

[19] S.M. Abdelkader, D.J. Morrow, "Online Thevenin equivalent determination considering system side changes and measurement errors,", IEEE Trans. Power Syst. 30 (5) (Sep. 2015) 2716–2725.

[20] P. Kundur, J. Paserba, V. Ajjarapu, G. Andersson, A. Bose, C. Canizares, N. Hatziargyriou, D. Hill, A. Stankovic, C. Taylor, T. van Cutsem, V. Vittal, "Definition and classification of power system stability,", IEEE Trans. Power Syst. 19 (2) (May 2004) 1387–1401.

[21] S. Corsi, G.N. Taranto, "Reliability analysis of voltage instability risk indicator based on a novel real-time identification algorithm,", Eur. Trans. Electr. Power 21 (4) (2011) 1610–1628.

[22] G.N. Taranto, C. Oyarce, S. Corsi, "Further investigations on a phasor measurement-based algorithm utilized for voltage stability awareness,", in: Proceedings of the IREP Symposium Bulk Power System Dynamics and Control - IX Optimization, Security and Control of the Emerging Power Grid, 2013.

[23] C.S. Carvalho, G.N. Taranto, "Comparison of voltage instability identification methods based on synchronized measurements,", in: Proceedings of the International Conference on Smart Grid Synchronized Measurements and Analytics (SGSMA), 2019.

[24] M.A. Pai, Energy Function Analysis for Power System Stability, Kluwer, MA, Norwell, 1989, pp. 223–227.